Vacuum wave function and mass gaps of U(1) lattice gauge theory in 2+1 dimensions

Xi-Yan Fang

China Center of Advanced Science and Technology (World Laboratory), P.O. Box 8730, Beijing 100080, China and Department of Physics, Zhongshan University, Guangzhou 510275, People's Republic of China

Jin-Ming Liu and Shuo-Hong Guo

Department of Physics, Zhongshan University, Guangzhou 510275, People's Republic of China

(Received 27 March 1995)

The nonperturbative coupled cluster method with the eigenvalue equations truncated in a scheme preserving the continuum limit is applied to Hamiltonian U(1) lattice gauge theory in 2+1 dimensions. The long wavelength vacuum wave function and mass gaps are calculated at orders 3, 4, 5, and 6. The results show nice scaling behaviors, and the values at the sixth order are in good agreement with theoretical expectations.

PACS number(s): 11.15.Ha

I. INTRODUCTION

In recent works [1, 2], a new nonperturbative method based on cluster expansion was put forward to study lattice gauge theory (LGT). The method consists of truncated eigenvalue equations with a specified truncation scheme that preserves the continuum limit. Our plan is to develop a systematic and effective analytical method to approach the scaling region. The (2+1)-dimensional [(2+1)D] SU(2) and SU(3) theories have been considered. As was expected, nice scaling behavior for the vacuum wave functions and mass gaps was obtained by this method even in low order calculations.

It is well known that SU(N) LGT in (2+1)D is superrenormalizable, and possesses a simple scaling property; that is, when the lattice spacing a goes to zero,

$$Ma \sim \text{const} \times g^2 \quad \text{as} \quad a \to 0, \tag{1.1}$$

where g is the dimensionless coupling constant. Hence, it is meaningful to apply the method to other situations with more complicated scaling behavior so as to test its effectiveness. The compact U(1) model in 2+1 dimensions is confining for all values of the coupling constant [3,4]. When the lattice spacing a goes to zero, the lattice mass gap Ma is expected to decrease exponentially [4]: that is:

$$M^2a^2 \sim \frac{c_1}{g^2}\exp\left(-\frac{c_2}{g^2}\right) \quad \text{as} \quad a \to 0. \tag{1.2}$$

Monte Carlo simulations have been used to study the Hamiltonian version of this model [5]. The results are consistent with Eq. (1.2). Some analytic investigations, which included variational researches [6–8], a block renormalization group study [9], and series analyses [10], also support the expected behavior. Therefore, this model, like SU(2) or SU(3) LGT in 3+1 dimensions, emerges as exponential scaling behavior in the weak coupling region, but it is much simpler than the latter. Hence, before we consider the (3+1)D theories, we first study the (2+1)D U(1) theory.

One of the major advantages of our method is that it is capable of giving the long wavelength vacuum wave function with correct scaling property [1,2]. Since (2+1)D U(1) LGT is a confining theory, we expect that its vacuum wave function has the same structure as that of SU(2) or SU(3) theory [see Eq. (2.10)]. The long wavelength expansion coefficient μ_0 and μ_2 will show exponential scaling in the U(1) case. The consistency of the exponential scaling properties of these coefficients and those of mass gaps will provide further evidence of the effectiveness of our method. Another reason for which we study this model is that the method may be used to study spin systems in condensed matter [11].

Our method is closely related to that of Refs. [12] and [13]. However, their truncation schemes violate the continuum limit, so that good scaling properties have not been obtained in their calculations.

This paper is organized as follows. In Sec. II, we introduce the truncation scheme and discuss the vacuum wave function. Section III is devoted to the calculation of the mass gaps. Our conclusions are presented in Sec. IV.

II. THE VACUUM WAVE FUNCTION

The Kogut-Susskind Hamiltonian in the model is

$$H = \frac{g^2}{2a}\sum_l E_l^2 - \frac{1}{2ag^2}\sum_p (U_p + U_p^\dagger), \tag{2.1}$$

where the index l denotes the links between sites, p labels the elementary plaquettes of the lattice, and a is the lattice spacing. Because of the confining property in this model, we suppose the form of the vacuum wave function is similar to that of SU(2) LGT [1, 2]: that is,

$$|\psi_0\rangle = e^{R(U)}|0\rangle, \tag{2.2}$$

where $R(U)$ consists of Wilson loops or linked clusters

and the state $|\,0\rangle$ is defined as

$$E_l\,|\,0\rangle = 0. \tag{2.3}$$

Defining a dimensionless operator

$$w = \frac{2a}{g^2}H = \sum_l E_l^2 - \frac{1}{g^4}\sum_p (U_p + U_p^\dagger), \tag{2.4}$$

the ground state eigenvalue equation is

$$\sum_l \left([E_l,[E_l,R]] + [E_l,R][E_l,R]\right) - \frac{1}{g^4}\sum_p (U_p + U_p^\dagger) = w_0, \tag{2.5}$$

where $w_0 g^2/2a$ is the ground state energy. The fundamental commutators are

$$[E_l, U_l] = U_l, \qquad [E_l, U_l^\dagger] = -U_l^\dagger. \tag{2.6}$$

Using Eq. (2.6), we get

$$[E_l,[E_l,U_l^n]] = n^2 U_l^n, [E_l,[E_l,U_l^{\dagger n}]] = n^2 U_l^{\dagger n},$$
$$[E_l,U_l][E_l,U_l] = U_l^2, [E_l,U_l][E_l,U_l^+] = -U_l U_l^+ = -1. \tag{2.7}$$

Let

$$[E_l,[E_l,G_i]] \equiv \mathrm{Dev}(G_i),$$

where G_i is any Wilson loop. From Eq. (2.7), we know G_i is an eigenvector of the operator Dev. For example,

$$\mathrm{Dev}\left([U_p(x)]^m[U_p(x+e_i)]^n\right) = (4m^2 + 4n^2 - 2mn)[U_p(x)]^m[U_p(x+e_i)]^n,$$

where $e_i (i = 1, 2)$ is a lattice vector with length a.

In general, like the case of SU(2) theory, the term $\sum_l [E_l, G_i][E_l, G_j]$ will produce new graphs which contain more plaquettes than those in G_i or G_j . Therefore, we expand R in order of graphs,

$$R = R_1 + R_2 + R_3 + \cdots, \tag{2.8}$$

and choose

$$R_1 = c_{1,1}\sum_x \left[U_p(x) + U_p^\dagger(x)\right] \equiv c_{1,1}(G_1 + G_1^+),$$

with a coefficient $c_{1,1}$ to be determined. R_1 is the lowest order term in R. The second order term is defined as a linear combination of all new graphs in $\sum_l [E_l, G_1 + G_1^\dagger][E_l, G_1 + G_1^\dagger]$, which are different from $G_1(G_1^+)$ and different from each other:

$$\begin{aligned} R_2 = {} & c_{2,1}\sum_x \left[U_p(x)U_p(x) + U_p^\dagger(x)U_p^\dagger(x)\right] \\ & + c_{2,2}\sum_{x,i}\frac{1}{2}\left[U_p(x)U_p(x+e_i) + U_p^\dagger(x)U_p^\dagger(x+e_i)\right] \\ & + c_{2,3}\sum_{x,i}\frac{1}{2}\left[U_p(x)U_p^\dagger(x+e_i) + U_p^\dagger(x)U_p(x+e_i)\right] \\ \equiv {} & \sum_s c_{2,s}(G_{2,s} + G_{2,s}^\dagger), \end{aligned}$$

where $c_{2,1}$, $c_{2,2}$, $c_{2,3}$ are coefficients to be determined. Similarly, we can obtain the higher order terms in R. The order of a graph defined by this procedure is not always equal to the number of plaquettes in the graph. For example, the graph

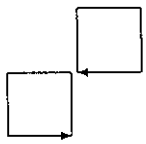

belongs to the fourth order, although it contains only two plaquettes.

Since $\sum_l [E_l, G_i][E_l, G_j] \subset G_{i+j}+$ lower order terms, we have to truncate Eq. (2.5). It is expected that the contribution of very high order graphs to low energy excited states is small. If the order in calculation were high enough, a different truncation scheme would give essentially the same result. However, it is difficult to include very high order terms in practical calculations. Then, an appropriate truncation scheme may soften the cutoff and lead to more rapid convergence to the scaling limit. Here, we adopt the continuum-limit-preserving scheme in Ref. [1]. In this scheme, the truncated eigenvalue equation at order n is

$$\sum_l \left(\left[E_l,\left[E_l,\sum_{i=1}^n R_i\right]\right] + \sum_{i+j\le n}[E_l,R_i][E_l,R_j]\right) - \frac{1}{g^4}\sum_p (U_p + U_p^\dagger) = w_0. \tag{2.9}$$

Comparing the coefficient of each independent graph on the two sides of Eq. (2.9), the values of $c_{i,s}$ and w_0 can be fixed. The essential feature of this truncation scheme is that it preserves the form of the continuum limit. Ignoring irrelevant constant terms, the continuum limit of a graph G_n is

$$G_n = e^2a^4[A_n \mathrm{Tr}F^2 + B_n a^2 \mathrm{Tr}(DF)^2 + \cdots],$$

where F is the field strength tensor, D the covariant derivative, and A_n and B_n are constants depending on the graph G_n. It was proved [1] that for any two graphs G_i and G_j, the continuum limit of the second term of Eq. (2.9) is

$$\sum_l [E_l, G_i][E_l, G_j] \sim -ke^2a^4\mathrm{Tr}(DF)^2,$$

where k is a constant depending on the graphs G_i and G_j. For the above continuum limit to hold, all graphs generated from that term must be included. Our truncated equation (2.9) satisfies the requirement and preserves the form of the continuum limit. It is expected that this scheme would lead to efficient approach to scaling.

The long wavelength vacuum wave function is

$$\psi(U) = N\exp\left[-\mu_0\int d^2x F^2 - \mu_2\int d^2x (D_iF)^2\right]. \tag{2.10}$$

Expanding U_p in order of a, we have

$$\mu_0 = g^2 a \sum_{i,s} A_{i,s} c_{i,s}, \quad \mu_2 = g^2 a^3 \sum_{i,s} B_{i,s} c_{i,s}, \tag{2.11}$$

with

$$A_{i,s} = (N_1 - N_2)^2,$$

$$B_{i,s} = -\frac{1}{2}\left[\left(\sum_{n=1}^{N_1} x_n^1 - \sum_{m=1}^{N_2} x_m^1\right)^2 + \left(\sum_{n=1}^{N_1} x_n^2 - \sum_{m=1}^{N_2} x_m^2\right)^2 + (N_2 - N_1) \times \left(\sum_{n=1}^{N_1}[(x_n^1)^2 + (x_n^2)^2] - \sum_{m=1}^{N_2}[(x_m^1)^2 + (x_m^2)^2]\right)\right], \tag{2.12}$$

where N_1 (N_2) is the number of oriented plaquettes U_p ($U_p^\dagger$) contained in the graph $G_{i,s}$, and (x_n^1, x_n^2) $(n = 1, \ldots, N_1)$ and (x_m^1, x_m^2) $(m = 1, \ldots, N_2)$ are the coordinates of the center points on plaquettes $U_p(x_n)$ and $U_p^+(x_m)$, respectively. Using Eq. (2.12), we can do all calculations on a computer.

Equation (1.2) leads to

$$ag = \frac{\sqrt{c_1}}{M} \exp\left(-\frac{c_2}{2g^2}\right) \quad \text{in the scaling region.} \tag{2.13}$$

Hence (in the scaling region)

$$2 \ln \frac{\mu_0}{ag} = 2 \ln \frac{\mu_0 M}{\sqrt{c_1}} + c_2 \frac{1}{g^2};$$

that is,

$$2 \ln(g A_{i,s} c_{i,s}) = 2 \ln \frac{\mu_0 M}{\sqrt{c_1}} + c_2 \frac{1}{g^2}. \tag{2.14a}$$

Similarly

$$\frac{2}{3} \ln\left(-\frac{B_{i,s} c_{i,s}}{g}\right) = \frac{2}{3} \ln\left(-\frac{\mu_2 M^3}{\sqrt{c_1^3}}\right) + c_2 \frac{1}{g^2}. \tag{2.14b}$$

Let

$$\mu_0' \equiv 2 \ln(g A_{i,s} c_{i,s}), \quad \mu_2' \equiv \frac{2}{3} \ln\left(-\frac{B_{i,s} c_{i,s}}{g}\right).$$

In the continuum limit, μ_0, μ_2, c_1, and c_2 should be constants, which means that the curves of μ_0' and μ_2' against $\frac{1}{g^2}$ will be straight lines in the scaling region.

We solve Eq. (2.9) with n=3, 4, 5, and 6. The numbers of graphs in these cases are 13, 66, 356, and 2456, respectively. Figures 1 and 2 give the results. We see that μ_0' shows good scaling in the interval $\frac{1}{g^2} \in [0.8, 1.6]$ at order 6. From this curve, we get

$$c_2 = 5.09(6), \qquad 2 \ln \frac{\mu_0 M}{\sqrt{c_1}} = -6.94(6). \tag{2.15a}$$

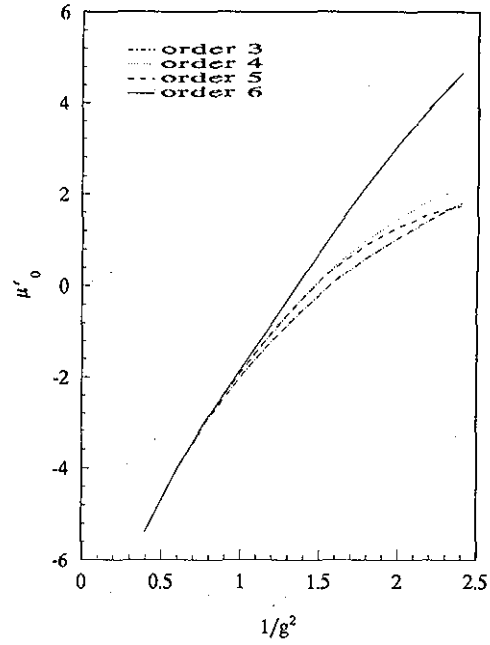

FIG. 1. The third to sixth order results of the coefficient μ_0' of the vacuum wave function as a function of $1/g^2$. The curve at sixth order shows nice scaling behavior.

The scaling behavior of μ_2' is not as good as μ_0'. This is not surprising, because μ_2 corresponds to higher order than μ_0 in the long wavelength expansion of $\psi(U)$. Since the scaling is improved gradually from the third order to the sixth order, it is possible to get better scaling for μ_2 at higher orders. Taking $c_2 = 5.09$, then, from Fig. 2, we

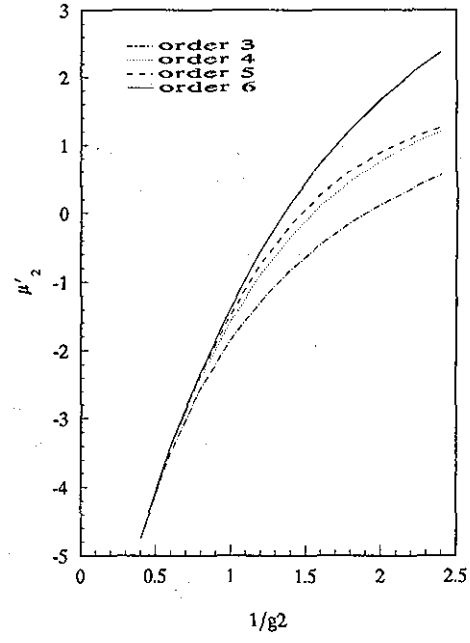

FIG. 2. The third to sixth order results of the coefficient μ_2' of the vacuum wave function as a function of $1/g^2$.

estimate

$$\frac{2}{3}\ln\left(-\frac{\mu_2 M^3}{\sqrt{c_1^3}}\right) \approx -6.39. \tag{2.15b}$$

III. MASS GAPS

In this section, we compute the mass gaps. The method is similar to the one in Ref. [1]. We take the glueball wave function as

$$|\psi\rangle = F(U)e^{R(U)}\,|\,0\rangle. \tag{3.1}$$

$F(U)$ contains various Wilson loops with the appropriate symmetry. Like $R(U)$, $F(U)$ is expanded according to the order of graphs:

$$F(U) = F_1 + F_2 + \cdots. \tag{3.2}$$

The nth order truncated eigenvalue equation is

$$\sum_l \left(\left[E_l, \left[E_l, \sum_{i=1}^{n} F_i\right]\right] + 2\sum_{i+j\le n}[E_l, F_i][E_l, R_j]\right) = \Delta w \sum_{i=1}^{n} F_i, \tag{3.3}$$

where $\Delta w g^2/2a$ is the glueball mass. We only do the calculation for the antisymmetric and symmetric lowest-lying excited states of the model under a parity transformation, denoted by M_A and M_S, respectively, in the following. The lowest order term in Eq. (3.2) is chosen to be

$$F_1^A = f_1^A \sum_p (U_p - U_p^\dagger) \quad \text{for } M_A,$$

$$F_1^S = f_1^S \sum_p (U_p + U_p^\dagger) \quad \text{for } M_S.$$

Higher order terms can be determined by the same method as in $R(U)$. Using Eq. (1.2), we deduce

$$\ln(M_A^2 a^2 g^2) \sim \ln c_1^A - c_2\frac{1}{g^2},$$

$$\ln(M_S^2 a^2 g^2) \sim \ln c_1^S - c_2\frac{1}{g^2}.$$

In Figs. 3 and 4, we present results of $\ln(M_A^2 a^2 g^2)$ and $\ln(M_S^2 a^2 g^2)$ against $\frac{1}{g^2}$ from the third order to the sixth order. The M_A curves show clearly the tendency to converge to the scaling limit. From the scaling window $1/g^2 \in [0.8, 1.2]$, we obtain

$$c_2 = 5.0(2), \qquad \ln c_1^A = 5.9(2). \tag{3.4}$$

The agreement of c_2 determined from the mass gap M_A and that from μ_0 [Eq. (2.15a)] is very impressive. These c_2 values are also in reasonable agreement with the results in Refs. [7–10].

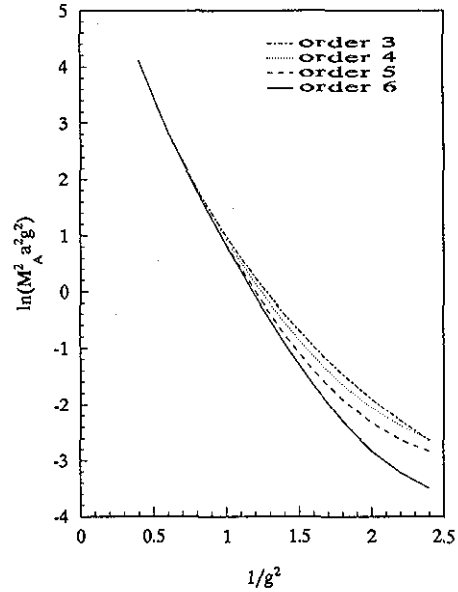

FIG. 3. The third to sixth order results of the mass gap M_A as a function of $1/g^2$. The curve at sixth order shows scaling behavior.

The scaling behavior for M_S is still not obtained in the sixth order approximation. One reason for the better scaling of M_A over that of M_S is that, because of symmetry, $|\,\psi_A\rangle$ is automatically orthogonal to the vacuum state $|\,\psi_0\rangle$, but $|\,\psi_S\rangle$ is in general not orthogonal to $|\,\psi_0\rangle$ in an approximate calculation. Hence, M_S is determined much less accurately than M_A. The second reason, which may be the more important one, is that theoretical consideration predicts $M_S = 2M_A$, so that the symmetric state (M_S) is not a compact glueball state, but it is composed of two free antisymmetric states. In order to obtain a good scaling behavior for M_S, we must go to higher or-

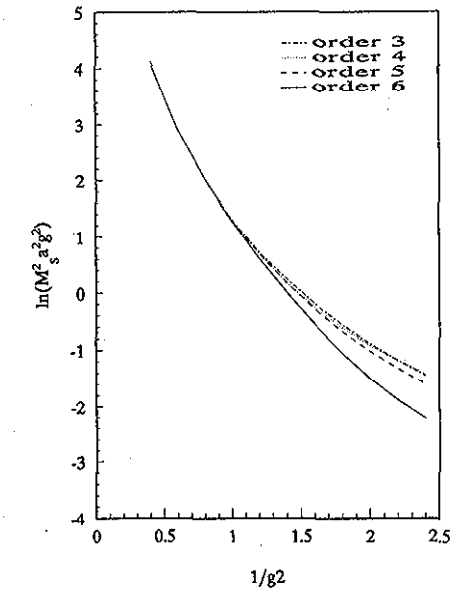

FIG. 4. The third to sixth order results of the mass gap M_S as a function of $1/g^2$.

der to see this composite structure. We think that this problem may be resolved in higher order calculations.

Using Eqs. (2.15) and (3.4), we get more concrete results:

$$\mu_0 M_A = 0.59(5), \quad \mu_2 M_A^3 \approx -0.48, \quad \text{and} \quad c_1^A = 365(73).$$

Because M_S does not show scaling behavior at the sixth order, the calculated ratio $\frac{M_S}{M_A}$ is not a constant in the weak coupling region. Nevertheless, from Figs. 3 and 4, $\frac{M_S}{M_A}$ is near 2.0 in that region, which is in reasonable agreement with the result in Ref. [9].

IV. CONCLUSIONS

In summary, we have applied the truncated eigenvalue equation method [1, 2] to (2+1)-dimensional U(1) LGT, and calculated the long wavelength vacuum wave function and the mass gaps. Our main results are

$$\frac{\mu_0}{a} = 3.11(9) \times 10^{-2} g \, \exp\left(2.54(3)\frac{1}{g^2}\right) \quad \text{as} \quad g^2 \to 0 \tag{4.1}$$

and

$$M_A^2 a^2 = \frac{365(73)}{g^2} \exp\left(\frac{-5.0(2)}{g^2}\right) \quad \text{as} \quad g^2 \to 0\,. \tag{4.2}$$

The μ_0 result has not been reported in the literature. The M_A result is to be compared with those obtained by other methods, which are the following .

(a) A variational estimate with

$$M_A^2 a^2 = \frac{500(30)}{g^2} \exp\left(\frac{-4.97(5)}{g^2}\right), \tag{4.3}$$

by Heys and Stump [7], and

$$M_A^2 a^2 = \frac{520(10)}{g^2} \exp\left(\frac{-4.80(6)}{g^2}\right), \tag{4.4}$$

by Dabringhaus, Ristig, and Clark [8].

(b) A block renormalization-group investigation with [9]

$$M_A^2 a^2 = \frac{145(15)}{g^2} = \exp\left(\frac{-4.1(2)}{g^2}\right). \tag{4.5}$$

(c) A series analysis with [10]

$$M_A^2 a^2 = \frac{529(30)}{g^2} \exp\left(\frac{-5.42(6)}{g^2}\right). \tag{4.6}$$

As for M_S, the results in above references are not so good as M_A (perhaps with the exception of Ref. [9]). This may be explained by the composite structure of the M_S state.

Besides, we also obtain

$$\mu_0 M_A = 0.59(5) \quad \text{and} \quad \mu_2 M_A^3 \approx -0.48. \tag{4.7}$$

We obtain nice scaling behavior at order $n = 6$. Comparing with this, $n = 3$ or 4 is sufficient in the case of 2+1 dimensional SU(2) and SU(3) LGT [1,2]. This shows that more complex configurations are needed to consider in the case of exponential scaling.

ACKNOWLEDGMENTS

This work was supported by the Doctoral Program Foundation of the Institute of Higher Education, People's Republic of China.

[1] S. H. Guo, O. Z. Chen, and L. Li, Phys. Rev. D **49**, 507 (1994); Q. Z. Chen, S. H. Guo, W. H. Zheng, and X. Y. Fang, *ibid.* **50**, 3564 (1994).

[2] Q. Z. Chen, X. Q. Luo, and S. H. Guo, Phys. Lett. B **341**, 349 (1995).

[3] A. M. Polyakov, Nucl. Phys. **B120**, 429 (1977).

[4] M. Cöpfert and G. Mack, Commun. Math. Phys. **82**, 545 (1982).

[5] D. W. Heys and D. R. Stump, Phys. Rev. D **28**, 2067 (1983); S. E. Koonin, E. A. Umland, and M. R. Zimbauer, *ibid.* **33**, 1795 (1986); C. M. Yang, C. R. Allton, and C. J. Hamer, *ibid.* **39**, 3778 (1989).

[6] D. Horn and M. Weinstein, Phys. Rev. D **25**, 3331 (1982); P. Suranyi, Phys. Lett. **122B**, 279 (1983); Nucl. Phys. **B225**, 77 (1983); H. Arisue, M. Koto, and T. Fujiwara, Prog. Theor. Phys. **229**, 70 (1983).

[7] D. W. Heys and D. R. Stump, Nucl. Phys. **B257**, 19 (1985); **B258**, 13 (1987).

[8] A. Dabringhaus, M. L. Ristig, and J. W. Clark, Phys. Rev. D **43**, 1978 (1991).

[9] G. Lana, Phys. Rev. D **38**, 1954 (1988).

[10] C. J. Hamer, J. Oitmaa, and W. H. Zheng, Phys. Rev. D **45**, 4652 (1992); A. C. Irving and C. J. Hamer, Nucl. Phys. **B230**, 361 (1984); **B235**, 358 (1984); C. J. Hamer and A. C. Irving, Z. Phys. C **27**, 145 (1985).

[11] R. F. Bishop, R. G. Hole, and Y. Xian, Phys. Rev. Lett. **73**, 3157 (1994); F. Petit and M. Roger, Phys. Rev. B **49**, 3453 (1994).

[12] R. F. Bishop, A. S. Kendall, L. Y. Wong, and Y. Xian, Phys. Rev. D **48**, 887 (1993).

[13] C. H. Llewellyn Smith and N. J. Watson, Phys. Lett. B **302**, 463 (1993).